Simultaneous directional emissions of multiple quantum emitters with cross plasmonic antenna

J. J. Yang,[1] S. M. Wang,[1,*] Q. Q. Cheng,[2] T. Li,[2] X. P. Hu,[1] and S. N. Zhu[1]

[1]*National laboratory of solid state microstructures, School of Physics, Nanjing University, Nanjing, China*
[2]*National laboratory of solid state microstructures, College of Engineering and Applied Sciences, Nanjing University, Nanjing, China*
**wangshuming@nju.edu.cn*

Abstract: We introduce a cross plasmonic antenna (CPA) for the system of multiple quantum emitters (QEs) with different emission wavelengths, where the excitation light scattering and emission fluorescence of different QEs are spatially separated in four different directions. By considering the CPA as oscillating dipoles, this phenomenon is attributed to the phase differences between them. The enhancement for QEs are very strong in correponding directions. In addition, the fluorescence is strongly polarized. By adding a silver plate as substrate, the directivity can be further tuned in the whole upper half space. Our result shows that the CPA is promising for realization of an efficient, directional and strongly polarized nano-scale light source, which will have potential application in Nano-Optics.

OCIS codes: (240.6680) Surface plasmons; (250.5403) Plasmonics; (260.2510) Fluorescence.

References and links

1. H. A. Atwater and A. Polman, "Plasmonics for improved photovoltaic devices," Nat. Mater. **9**(3), 205–213 (2010).
2. Z. Liu, W. Hou, P. Pavaskar, M. Aykol, and S. B. Cronin, "Plasmon Resonant Enhancement of Photocatalytic Water Splitting Under Visible Illumination," Nano Lett. **11**(3), 1111–1116 (2011).
3. M. Wang, M. Yang, J. Cheng, J. Dai, M. Yang, and D. N. Wang, "Femtosecond laser fabricated micro Mach-Zehnder interferometer with Pd film as sensing materials for hydrogen sensing," Opt. Lett. **37**(11), 1940–1942 (2012).
4. M. Labidi, J. B. Tahar, and F. Choubani, "Meta-materials applications in thin- film sensing and sensing liquids properties," Opt. Express **19**(S4 Suppl 4), A733–A739 (2011).
5. M. L. Juan, R. Gordon, Y. Pang, F. Eftekhari, and R. Quidant, "Self-induced back-action optical trapping of dielectric nanoparticles," Nat. Phys. **5**(12), 915–919 (2009).
6. W. Zhang, L. Huang, C. Santschi, and O. J. F. Martin, "Trapping and Sensing 10 nm Metal Nanoparticles Using Plasmonic Dipole Antennas," Nano Lett. **10**(3), 1006–1011 (2010).
7. A. Kinkhabwala, Z. Yu, S. Fan, Y. Avlasevich, K. Mullen, and W. Moerner, "Large single-molecule fluorescence enhancements produced by a bowtie nanoantenna," Nat. Photonics **3**(11), 654–657 (2009).
8. H. Harutyunyan, G. Volpe, R. Quidant, and L. Novotny, "Enhancing the nonlinear optical response using multifrequency gold-nanowire antennas," Phys. Rev. Lett. **108**(21), 217403 (2012).
9. R. Czaplicki, H. Husu, R. Siikanen, J. Mäkitalo, M. Kauranen, J. Laukkanen, J. Lehtolahti, and M. Kuittinen, "Enhancement of Second-Harmonic Generation from Metal Nanoparticles by Passive Elements," Phys. Rev. Lett. **110**(9), 093902 (2013).
10. A. V. Akimov, A. Mukherjee, C. L. Yu, D. E. Chang, A. S. Zibrov, P. R. Hemmer, H. Park, and M. D. Lukin, "Generation of single optical plasmons in metallic nanowires coupled to quantum dots," Nature **450**(7168), 402–406 (2007).
11. Z. Jacob and V. M. Shalaev, "Physics. Plasmonics Goes Quantum," Science **334**(6055), 463–464 (2011).
12. K. H. Drexhage, *Progress in Optics* (North-Holland, 1974), Vol. XII, p. 165–232.
13. H. Yokoyama and K. Ujihara, *Spontaneous Emission and Laser Oscillation in Microcavities* (CRC Press, 1995).
14. P. R. Berman, *Cavity Quantum Electrodynamics* (Academic Press, 1994).
15. S. Noda, M. Fujita, and T. Asano, "Spontaneous-emission control by photonic crystals and nanocavities," Nat. Photonics **1**(8), 449–458 (2007).
16. B. Rolly, B. Stout, S. Bidault, and N. Bonod, "Crucial role of the emitter-particle distance on the directivity of optical antennas," Opt. Lett. **36**(17), 3368–3370 (2011).
17. J. M. Geffrin, B. García-Cámara, R. Gómez-Medina, P. Albella, L. S. Froufe-Pérez, C. Eyraud, A. Litman, R. Vaillon, F. González, M. Nieto-Vesperinas, J. J. Sáenz, and F. Moreno, "Magnetic and electric coherence in

#236379 - $15.00 USD Received 20 Mar 2015; revised 28 May 2015; accepted 28 May 2015; published 1 Jun 2015

forward- and back-scattered electromagnetic waves by a single dielectric subwavelength sphere," Nat. Commun. **3**, 1171 (2012).
18. S. Kühn, U. Håkanson, L. Rogobete, and V. Sandoghdar, "Enhancement of single-molecule fluorescence using a gold nanoparticle as an optical nanoantenna," Phys. Rev. Lett. **97**(1), 017402 (2006).
19. L. Novotny and N. van Hulst, "Antennas for light," Nat. Photonics **5**(2), 83–90 (2011).
20. X. W. Chen, M. Agio, and V. Sandoghdar, "Metallodielectric Hybrid Antennas for Ultrastrong Enhancement of Spontaneous Emission," Phys. Rev. Lett. **108**(23), 233001 (2012).
21. X. Zeng, W. Yu, P. Yao, Z. Xi, Y. Lu, and P. Wang, "Metallo-dielectric hybrid antenna for high Purcell factor and radiation efficiency," Opt. Express **22**(12), 14517–14523 (2014).
22. H. Aouani, O. Mahboub, N. Bonod, E. Devaux, E. Popov, H. Rigneault, T. W. Ebbesen, and J. Wenger, "Bright unidirectional fluorescence emission of molecules in a nanoaperture with plasmonic corrugations," Nano Lett. **11**(2), 637–644 (2011).
23. Z. Xi, Y. Lu, W. Yu, P. Yao, P. Wang, and H. Ming, "Tailoring the directivity of both excitation and emission of dipole simultaneously with two-colored plasmonic antenna," Opt. Express **21**(24), 29365–29373 (2013).
24. A. G. Curto, G. Volpe, T. H. Taminiau, M. P. Kreuzer, R. Quidant, and N. F. van Hulst, "Unidirectional Emission of a Quantum Dot Coupled to a Nanoantenna," Science **329**(5994), 930–933 (2010).
25. H. Aouani, O. Mahboub, E. Devaux, H. Rigneault, T. W. Ebbesen, and J. Wenger, "Plasmonic Antennas for Directional Sorting of Fluorescence Emission," Nano Lett. **11**(6), 2400–2406 (2011).
26. T. Shegai, S. Chen, V. D. Miljković, G. Zengin, P. Johansson, and M. Käll, "A bimetallic nanoantenna for directional colour routing," Nat. Commun. **2**, 481 (2011).
27. T. Kosako, Y. Kadoya, and H. F. Hofmann, "Directional control of light by a nano-optical Yagi-Uda antenna," Nat. Photonics **4**(5), 312–315 (2010).
28. Y. C. Jun, K. C. Y. Huang, and M. L. Brongersma, "Plasmonic beaming and active control over fluorescent emission," Nat. Commun. **2**, 283 (2011).
29. F. Bigourdan, F. Marquier, J.-P. Hugonin, and J. J. Greffet, "Design of highly efficient metallo-dielectric patch antennas for single-photon emission," Opt. Express **22**(3), 2337–2347 (2014).
30. T. Coenen, F. Bernal Arango, A. Femius Koenderink, and A. Polman, "Directional emission from a single plasmonic scatterer," Nat. Commun. **5**, 3250 (2014).
31. T. Pakizeh and M. Käll, "Unidirectional ultracompact optical nanoantennas," Nano Lett. **9**(6), 2343–2349 (2009).
32. T. Taminiau, F. Stefani, F. Segerink, and N. Van Hulst, "Optical antennas direct single-molecule emission," Nat. Photonics **2**(4), 234–237 (2008).

Light-matter interaction, for example, the absorption and emission of light as well as the control of its spectral and directional properties, is a key element for a wide range of applications, from solar energy conversion [1,2], sensing applications [3,4], single-particle manipulation [5,6], spectroscopy [7], enhancing nonlinear optical response [8,9], and quantum information processing [10,11]. Spontaneous emission of quantum emitter (QE), fluorescent molecules or quantum dots, is radiated along all directions which severely limits the amount of collected light. It is of great significance and remains a challenge to enhance the emission rate and control the fluorescence directivity. To achieve this, a lot of efforts have been focused on flat interfaces [12], and Fabry-Perot resonators [13,14], while other works have considered structured dielectric structures [15] and nanoparticles [16–18] which are called optical antennas [19]. In particular, plasmonic nanoantennas can optimize the absorption and emission of light [7,20,21] as well as the control of its spectral and directional properties [22–32].

Earlier works have realized unidirectional emission of a single emitter by coupling to a Yagi-Uda antenna [24,27], in which the resulting quantum dot fluorescence is strongly polarized and highly directed into a narrow forward angular cone. It has been discovered that the directivity of emitters is sensitive to the distance between the emitter and the gold nanoparticle [16], which is due to rapid phase variations of the emitter field at short distances. And gold nanoapertures surrounded by periodic corrugations can transform standard fluorescent molecules into bright unidirectional sources [22], which can also been used for directional sorting of fluorescence emission [25]. It can be seen that plasmonic antennas can enhance the emission rate of QEs greatly and control the direction conveniently.

Recently, a two-colored plasmonic antenna is designed to control the directivity of the excitation and emission light independently and simultaneously [23]. By tuning the phase difference between different unit nanoparticles of the antenna, the excitation and emission direction of a single fluorescent molecule can be spatially separated and manipulated independently, which is very important for fluorescence collection. However, this kind of

#236379 - $15.00 USD Received 20 Mar 2015; revised 28 May 2015; accepted 28 May 2015; published 1 Jun 2015

antenna cannot be used for system of multiple QEs with different emission wavelengths. To achieve this, we must have more than two resonances corresponding to the excitation and emission wavelengths of multiple QEs in the plasmonic antenna. Here, we come up with a cross plasmonic antenna (CPA) with four resonances at different wavelengths, where the excitation light scattering and emission fluorescence of three different kinds of QEs can be separated in four different directions. The enhancement factor for the QEs in corresponding directions are very large compared with that of an isolated emitter and the fluorescence is strongly polarized. Moreover, by adding a silver plate as substrate, the directivity of CPA can be further tuned in any direction in the upper half space, which increases the tunability of the CPA.

We introduce the CPA containing four resonances corresponding respectively to the excitation and emission wavelengths of the QEs, so that both the pumping field and emission can be enhanced. The CPA is shown in Fig. 1(a), which consists of four pairs of silver nanorods sharing one same nanorod in the middle. The excitation field is shown in Fig. 1(b), by which four evident resonances can be excited. By measuring the magnetic field Hz in the middle of space between nanorods 0 and 1 and between nanorods 0 and 2, we obtain two resonant wavelengths $\lambda_1 = 798nm$ *and* $\lambda_2 = 656nm$. Similarly, by measuring the magnetic field Hx in the middle of space between nanorods 0 and 3 and between nanorods 0 and 4, we obtain another two resonant wavelengths $\lambda_3 = 594.5nm$ *and* $\lambda_4 = 563nm$. The resonant wavelengths can be seen in Fig. 1(c). The distribution of magnetic field and electric field at four resonant wavelengths are shown in Fig. 1(d). The resonance strongly depends on the distance between metallic nanorods. By increasing the gap between nanoparticles, the interaction between them decreases, and the resonant frequency increases. If the aspect ratio of the nanorod increases (with increased L/a), its resonance shifts to longer wavelength. Therefore, the CPA can apply to system of QEs with other different frequencies by simply varying its size. The QE can be simulated by a y-direction short current source placed 10nm above the shared nanorod of the four nanorods. The spatial overlap of four resonances which introduce strong field enhancement can enhance the fluorescence in both excitation and emission.

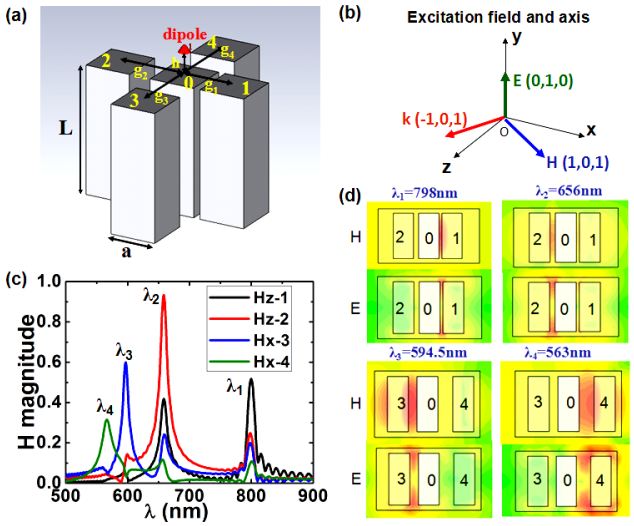

Fig. 1. (a) The structure of the CPA with a = 40nm, L = 100nm, g_1 = 46nm, g_2 = 50nm, g_3 = 56nm, g_4 = 68nm, h = 10nm. The CPA is immersed in air. (b) The excitation field and coordinate axis. (c) Resonance of the antenna by measuring the magnetic field Hz in the middle of space between nanorods 0 and 1, 0 and 2, and Hx in the middle of space between nanorods 0 and 3, 0 and 4 of the antenna. (d) The magnetic field and electric field distribution at four resonances.

#236379 - $15.00 USD Received 20 Mar 2015; revised 28 May 2015; accepted 28 May 2015; published 1 Jun 2015

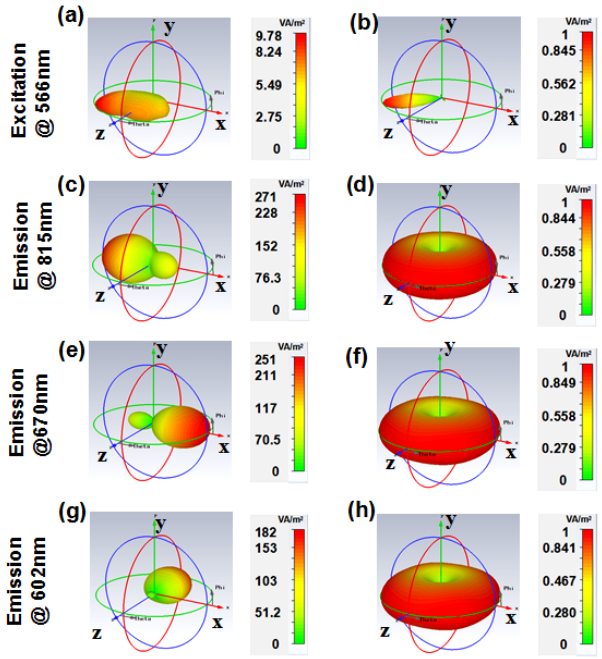

Fig. 2. The far-field pattern plot at excitation and emission wavelengths of the QEs in presence of CPA (a,c,e,g) and of that in vacuum (b,d,f,h). The size of the CPA is a = 40nm, L = 100nm, g_1 = 46nm, g_2 = 50nm, g_3 = 56nm, g_4 = 68nm, h = 10nm. The scale bar of power is shown in the figure.

The excitation and emission of the antenna is simulated by CST Microwave Studio and the permittivity of silver has Drude model $\varepsilon = \varepsilon_\infty - \omega_p^2/(\omega^2 - i\gamma\omega)$ with $\varepsilon_\infty = 1.0$, $\omega_p = 1.37 \times 10^{16} rad/s$, $\gamma = 1.95 \times 10^{12} rad/s$. We choose silver nanorod with square cross section as the building block of CPA because silver nanorod exhibits higher fluorescent enhancement than gold. As a comparison, the QE in vacuum is also studied. The angular distribution pattern at excitation wavelength is simulated by radiating the antenna with plane wave then detecting the scattered power distribution in the far field. The emission pattern is obtained in a similar way by exciting the antenna with a dipole source near the antenna. Combining both the excitation and emission enhancement effect, the total enhancement factor for QE with different emission wavelength λ_{em} in the direction (θ,ϕ) is defined as [23]:

$$S(\theta,\varphi) = \frac{P(\theta,\varphi,\lambda_{em})}{Max\left(P_0(\theta,\varphi,\lambda_{em})\right)} \times \frac{\left|E_{y,\lambda_{ex}}\right|^2}{\left|E_{0,\lambda_{ex}}\right|^2}, \tag{1}$$

where $P(\theta,\phi,\lambda_{em})$ is the angular distribution of the emitted power with CPA and $P_0(\theta,\phi,\lambda_{em})$ is the angular distribution of the emitted power by an isolated source in vacuum. The ratio represents the angular radiative emission enhancement of quantum emitter in presence of the CPA. It is not the ratio between the total fluorescence of QE with CPA and that of an isolated emitter distributed over all directions, which is related to the decay rate enhancement of QE with CPA. The multiplier term $|E_{y,\lambda ex}|^2/|E_{0,\lambda ex}|^2$ incorporates the enhancement at the excitation wavelength, which is close to the ratio of excitation scattering power with CPA to that in vacuum. Thus, the total enhancement factor S(θ,ϕ) is the product of angular enhancement of emission and the enhancement of the excitation.

Figure 2 presents the far-field radiation and excitation pattern of QE in presence of CPA and of that in vacuum. For the excitation and emission of QE with CPA, the emitted power is

#236379 - $15.00 USD Received 20 Mar 2015; revised 28 May 2015; accepted 28 May 2015; published 1 Jun 2015

reflected from (−1,0,1) direction resulting directional emissions in -x direction, + x direction, -z direction (Figs. 2(b-d)). Whereas the direction of the scattered power mainly resides in the + z direction (Fig. 2(a)) resulting in a highly asymmetric pattern. This is strikingly different from the emission of an isolated emitter, which is classical doughnut pattern with evenly distributed power in the xz plane (Figs. 2(f-h)). This is because the nanorods undergo large phase variation due to plasmonic hybridization [17,26,31], the strong near field interaction of the anti-phase magnetic resonant mode provide different far-field pattern. What's more, the far-field power with CPA is greatly enhanced compared with an isolated emitter. In the scale bar of power in Figs. 2(e-h), the maximum powers of excitation and emission patterns of an isolated emitter are all taken to be 1 at corresponding wavelengths. In Figs. 2(a-d), the power with CPA is normalized to the maximum power of an isolated emitter at corresponding wavelength. In this way, the value in the scale bar is just the enhancement of excitation or emission of QE with CPA compared with an isolated emitter in corresponding directions. We can see that the maximum angular enhancement of the emission for three QE is around 200 and that of the excitation is about 10. Thus, the maximum S factors in emission directions are about 2000.

The observed directivity in CPA arises from interference between nanorods composing the antenna. When the quantum emitter is effectively coupled to the antenna, its far field pattern is dominated by the antenna [32]. Without loss of generality, we take the CPA as two oscillating dipoles with phase differences [23]. For the excitation process at $\lambda_4 = 566nm$, we discuss the case nanorods 0 and 4 are at resonance. For the emission process at $\lambda_1 = 815nm$ ($\lambda_2 = 670nm$, $\lambda_3 = 602nm$), the nanorods 0 and 1 (2, 3) are at resonance. The total far field electric field is the vectorial summation of the individual nanorod with dipole moment $\vec{p}_d = |p_d| e^{i\varphi_d}$,

$$\vec{E}_{tot} = \sum_{d=i}^{j} \left(\frac{\omega}{c}\right)^2 \frac{1}{4\pi\varepsilon_0} e^{ik(\vec{r}-\vec{x}_d)} (\vec{e}_r \times \vec{p}_d) \times \vec{e}_r, \tag{2}$$

with $i = 0, j = 4$ for the excitation process and $i = 0, j = 1, 2, 3$ for the emission process. Since we are only interested in the symmetry of the power pattern, we compute the sum of Poynting vectors in + z and -z direction and that in + x and -x directions which yield to [16]:

$$\Delta\vec{P}_z = \vec{P}_{+z} + \vec{P}_{-z} = \frac{\omega^3 k |p_i||p_j|}{8\pi^2 \varepsilon_0 c^2 r^2} \sin(\varphi_{ij}) \sin(kd)\, \vec{z}, \tag{3}$$

$$\Delta\vec{P}_x = \vec{P}_{+x} + \vec{P}_{-x} = \frac{\omega^3 k |p_i||p_j|}{8\pi^2 \varepsilon_0 c^2 r^2} \sin(\varphi_{ij}) \sin(kd)\, \vec{x}, \tag{4}$$

with ϕ_{ij} being the phase difference between the two nanorods. For small distance d between nanorods, the change of $sin(\phi_{ij})$ will induce change in the radiation symmetry. Obviously, when ϕ_{ij} is the odd multiples of $\pi/2$, we will obtain directional excitation and emission pattern. At the excitation frequency $\lambda_4 = 566nm$, the phase difference $\phi_{04} = \pi/2$ and the incident light preferentially scatters into + z direction. At the emission frequency $\lambda_1 = 815nm$ ($\lambda_2 = 670nm$, $\lambda_3 = 602nm$), the phase difference $\phi_{01} = -\pi/2$, ($\phi_{02} = \pi/2$, $\phi_{03} = -\pi/2$) and the emission lies mainly in -x (+ x, -z) direction. We can see that the excitation and emission wavelengths are around the four resonant wavelengths, which is due to large phase variations near magnetic resonances.

#236379 - $15.00 USD Received 20 Mar 2015; revised 28 May 2015; accepted 28 May 2015; published 1 Jun 2015

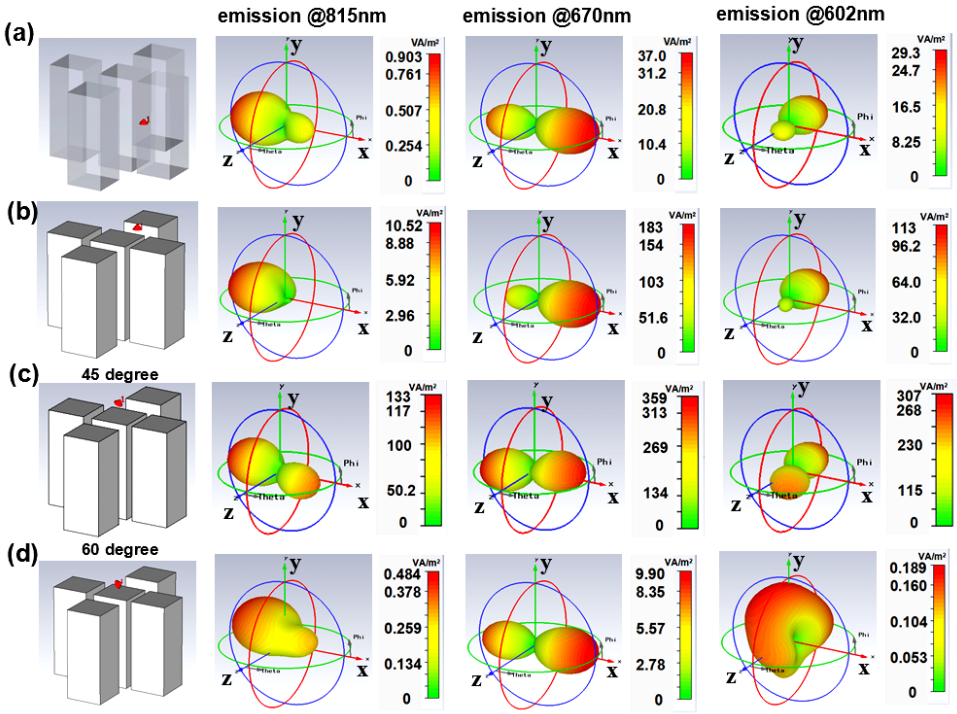

Fig. 3. The influence of changing the position and orientation of the dipole. The emission pattern when the dipole is in the middle of nanorod 0 and nanorod 1 in (a), above the center of nanorod 0 and nanorod 1 in (b), when its orientation is 45 degree to the y-axis in (c), and 60 degree to the y-axis in (d). The scale bar of power is shown in the figure.

We know that the fluorescence of QE is not polarized. However, in some cases we need polarized light source. Thus, we consider the polarization of the emission light of CPA here. We find that the emission and scattering field are strongly polarized. This is because the magnetic resonant modes are excited in CPA. Therefore, we obtain a directional and strongly polarized nano-scale light source. It will have a lot of applications in quantum information and plasmonic devices. Next, we have analyzed the influence of the position and orientation of the dipole on the emission power pattern. The result is shown in Fig. 3, where the power of emission pattern has been normalized to the maximum power of an isolated emitter at corresponding wavelength. First, we change the position of the dipole as shown in Figs. 3(a) and 3(b). We can see that the emission light still lies mainly in three different directions. In Fig. 3(b), the enhancement is larger and the directivity is better than that in Fig. 3(a). The reason for a larger enhancement is that the electric field is stronger near the top of the antenna than in the gap. When the dipole is placed above the antenna, it can excite the four resonances more efficiently which induces a better directivity. Then we change the orientation of the dipole as shown in Figs. 3(c) and 3(d). It also can be seen in Fig. 3(c) that the emission are still spatially separated in three different directions when the angle to the y-axis is 45 degree. The directivity is weakened in the emission directions while the enhancement does not change much. When the angle is 60 degree, the directivity of emission in -z direction is lost and the enhancement is very small. We conclude that CPA has a good performance within ± 45 degree to the y-axis. When it exceeds 45 degree, the directivity at some wavelengths will be lost and the enhancement will be decreased.

#236379 - $15.00 USD Received 20 Mar 2015; revised 28 May 2015; accepted 28 May 2015; published 1 Jun 2015

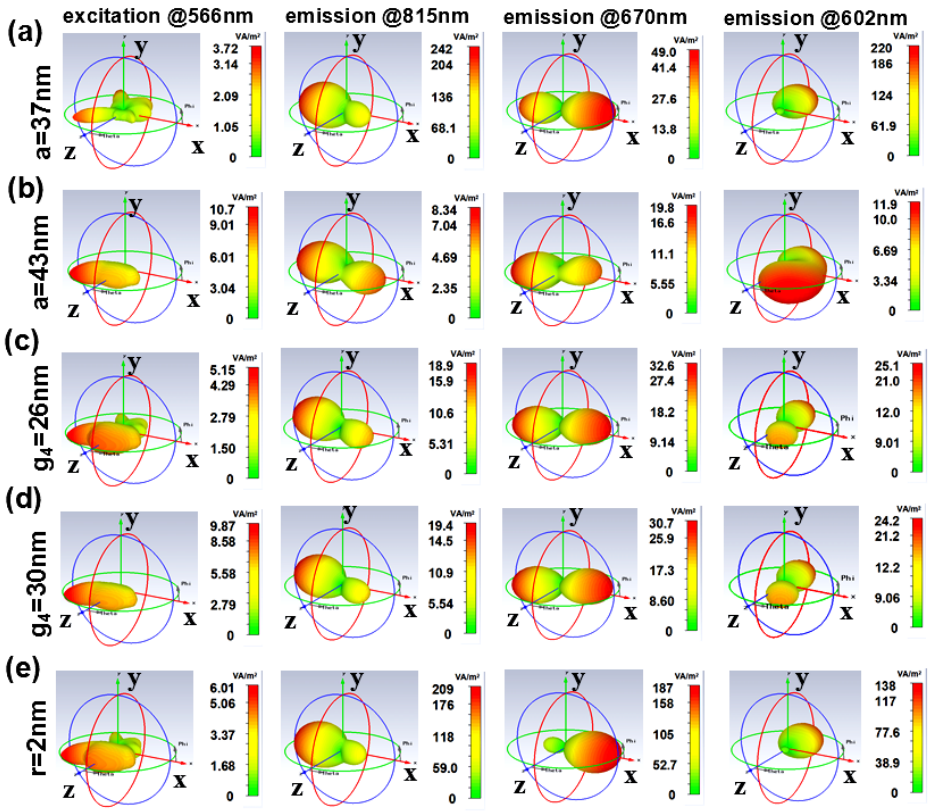

Fig. 4. The influence of changing the size of the structure on the far-field power pattern at excitation and emission wavelengths. The width of the nanorods is changed to a = 37nm in (a) and to 43nm in (b). The gap g_4 between nanorod 0 and nanorod 4 is changed to g_4 = 26nm in (c) and g_4 = 30nm in (d). (e) The nanorods are smoothed at both the lateral and top rectangular edges, the blending radius is r = 2nm. The scale bar is shown in the figure.

After that, the effect of variability in size and structure of the antenna on the performance of CPA has been considered in Fig. 4. Firstly, we change the width $a = 40nm$ of nanorods to 37nm (Fig. 4(a)) and 43nm (Fig. 4(b)). And we change the gap between nanorods 0 and 4 from $g_4 = 28nm$ to 26nm (Fig. 4(c)) and 30nm (Fig. 4(d)). The results can be seen in Fig. 4, where the power of excitation and emission pattern has also been normalized to the maximum power of an isolated emitter at corresponding wavelength. When $a = 37nm$ (Fig. 4(a)), the directivity and the enhancement of emission is decreased at 670nm and the directivity at excitation wavelength is lost. In Fig. 4(b), the enhancement of the emission at three wavelengths is decreased and directivity is not good at 670nm and 602nm when $a = 43nm$. In Figs. 4(c-d), the direcitivity at some wavelengths is weakened and the enhancement for three wavelengths is decreased, while the function of the antenna can be preserved when $g_4 = 26nm$ *and* $30nm$. Considering the fabrication error, we have smoothed all the rectangular edges of the nanorods in Fig. 4(e). The blending radius is taken to be $r = 2nm$. In this situation, the performance of the antenna is well preserved, in which the directivity is very good and the S factor is also very large. In these situations, the variability in size and structure of CPA has changed the resonance wavelenths, influencing the directivity and enhancement of the power pattern at excitation and emission wavelenghs. From these calculations, the CPA can be tolerant to the variability of size and structure of CPA to some extent.

#236379 - $15.00 USD Received 20 Mar 2015; revised 28 May 2015; accepted 28 May 2015; published 1 Jun 2015

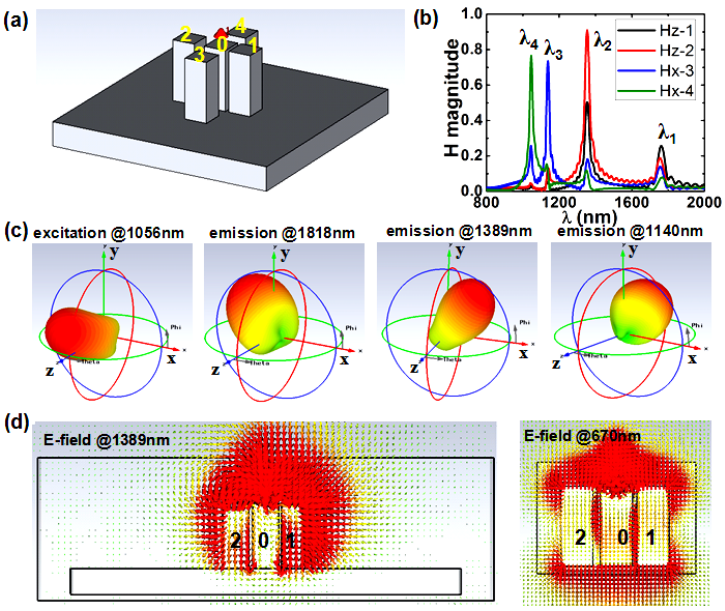

Fig. 5. Tuning the directivity of emission and excitation by adding a silver plate as substrate. (a) The structure of the antenna, with g_1 = 44nm, g_2 = 46nm, g_3 = 52nm, g_4 = 59nm, L = 100nm, a = 40nm, the size of the silver plate is 600nm × 40nm × 600nm. (b) The resonance of the structure at λ_1 = 1764nm, λ_2 = 1352nm, λ_3 = 1127nm and λ_4 = 1045nm. (c) The far-field pattern of excitation and emission. (d) The electric field of the structure in (a) at λ = 1389nm and the electric field of the structure in Fig. 1(a) at λ = 670nm.

We see that although the proposed CPA has a directional scattering as well as a directional emission property, the directivity is mainly limited in xz plane. We can tailor the emission and excitation directivities by adding a silver plate as substrate in Fig. 5(a). We have changed the gap between nanorods while the size of them is invariant. By adding a silver plate, the wavelength of the resonances shifted to longer wavelengths as the electromagnetic circuit lengthens. This kind of antenna applies to QEs with a longer wavelenth. The resonance wavelengths are $\lambda_1 = 1764nm$, $\lambda_2 = 1352nm$, $\lambda_3 = 1127nm$ and $\lambda_4 = 1045nm$ as shown in Fig. 5(b). In this way, we can make the emission and excitation directivity have more tunability, where the directivity can be tuned in the upper half space as shown in Fig. 5(c). This is because the silver plate can be seen as a mirror to reflect the electromagnetic field in + y direction. For example, we give the electric field distribution of CPA with and without a silver plate in Fig. 5(d) at wavelengths where nanorod 0 and nanorod 2 are at resonance, where we find that the silver plate introduces asymmetry of electric field in y-direction which is stronger in upper space. The silver plate pushed the electric field to make the antenna emit in + xy direction. By changing the size of the antenna, we can tune the emission and excitation directivity conveniently. In addition, we find that although the proposed CPA has a directional scattering and directional emission property, the directivity is less than traditional Yagi-Uda antenna [24,27]. However, the small size and the multiple emissions of CPA make it promising for high integration applications compared with traditional antennas. To improve the directivity of the CPA, antenna arrays can be used [23].

In conclusion, we have introduced a novel plasmonic antenna structure, the CPA, which can spatially separate the excitation and emission pattern in four different directions. And the emission light is strongly polarized. The directivity can be tuned in the upper half space by adding a silver plate as substrate. In this paper, the material around the CPA is taken to be air. The CPA has some tolerance to the position and direction of the dipole as well as to the variability in the size and structure of the antenna. Thus in real situation, we can immerse the

#236379 - $15.00 USD Received 20 Mar 2015; revised 28 May 2015; accepted 28 May 2015; published 1 Jun 2015

antenna in PMMA with QEs dispersed in it. The antenna will behave with large angular enhancement facotr and the frequency can be tuned by changing the size of it. What's more, it can be also used in system with one kind of QEs to obtain directional and very strong emission enhancement of quantum emitters with broadband excitation light which scattered in three different directions. We believe our findings can broaden the diversity of plasmonic devices. It can be used in directional and bright light sources for quantum optical technologies, biochemical sensors, light-harvesting and emission devices. This finding can also have potential applications in nanolaser and nonlinear process like second harmonic generation [8,9] where active control of excitation and emission pattern is necessary.

Acknowledgment

This work is supported by the National Key Projects of Basic Researches in China (Nos. 2012CB933501, 2012CB921802 and 2011CBA00205), the National Natural Science Foundation of China (Nos. 11322439, 11321063, 91321312).

#236379 - $15.00 USD Received 20 Mar 2015; revised 28 May 2015; accepted 28 May 2015; published 1 Jun 2015